Scanning Tunneling Microscopy, Tunneling Spectroscopy, and Photoelectrochemistry of a Film of Q-CdS Particles Incorporated in a Self-Assembled Monolayer on a Gold Surface

Shuichiro Ogawa, Fu-Ren F. Fan, and Allen J. Bard*

Department of Chemistry and Biochemistry, The University of Texas at Austin, Austin, Texas 78712

Received: February 22, 1995; In Final Form: May 13, 1995[⊗]

Films of AOT-capped (AOT = dioctyl sulfosuccinate) cadmium sulfide nanoparticles (Q-CdS) prepared by incorporation into a self-assembled monolayer (SAM) of hexanethiol on Au were prepared. These were imaged at negative substrate bias in air by scanning tunneling microscopy, and Q-CdS particles were shown to cover most of the area on the SAM. Continuous scanning of the tip over the substrate removed Q-CdS particles to the outside of the scanning area because of tip-substrate interactions. Scanning tunneling spectroscopy was carried out in air with the tip held over the thin CdS film (100 nm) and over individual Q-CdS particles in the layer. The i vs V and di/dV vs V curves indicated that the energy band gap of the Q-CdS particles is wider than that of the thin CdS films. The results of photoelectrochemistry also indicated that the onset photopotential is more negative for smaller Q-CdS particles and is related to the level of conduction band.

Introduction

Research on semiconductor electrodes[1] is driven by potential applications in electronics, electrooptics, imaging science, and photoelectrochemical (PEC) cells. Although there have been many studies with bulk semiconductor electrodes (single crystal and polycrystalline), there are fewer papers dealing with electrodes made of thin films of semiconductor nanoparticles (quantum or Q-particles).[2-5] Semiconductor nanoparticles have been the subject of a number of investigations concerning methods of preparation, stabilization, characterization, and the effect of particle size on the material properties.[6] Of particular interest has been the effect of particle size on the band gap energy (E_g) as measured by the absorption onset: in general, the smaller the particle, the larger the E_g and the shorter the wavelength for the onset of absorption. This phenomenon is called the quantum size effect. Many studies have involved studying changes in the optical, electrochemical (EC), PEC, and electrical properties of Q-particles by controlling their size, but these have mainly dealt with spectroscopic investigations of Q-particle dispersions (as opposed to films of particles on electrically conductive substrates).

Several methods of preparing thin films of nanoparticles, e.g., by self-assembly,[7] electrophoretic deposition,[8] chemical deposition,[9] electrochemical deposition,[10] or the Langmuir-Blodgett technique,[11-13] have been described. Some of these films contained very well-defined, close-packed particle layers and involved studies of the EC and PEC properties of Q-particle layers.[5,14] Particle size and film structure of Q-particle layers were usually studied by transmission electron microscopy (TEM) and scanning tunneling microscopy (STM).[3,15] The topographic self-assembled monolayers (SAMs), such as alkanethiol layers on gold, have also been studied by STM.[16] By combining STM with tunneling spectroscopy (TS),[17] the surface electronic properties of several semiconductors, such as Si,[18] GaAs,[19] and TiO_2,[20] have also been studied. Measurements of density of state distributions and E_g values of semiconductor surfaces have been reported. Fendler and co-workers have also studied quantized CdSe particulate films,[21] prepared with dioctadecyldimethylammonium bromide (DODAB), and CdS particulate films,[14] generated at an arachidic acid monolayer interface, by STM and TS. From these studies, they obtained information about the electronic structure of the size-quantized particles in the semiconductor film.

There are fewer papers concerning PEC studies of Q-particles.[10b,14,22] For example, of particular interest is the dependence of the potential for onset of the photocurrent, V_{on}, on the size of Q-particles and E_g. In principle, such PEC measurements of Q-particles, e.g., as films on electrodes, can provide information about the energies of the band edges and surface states, as frequently employed with bulk semiconductor electrodes.[1] Theoretically, V_{on} of Q-particles might be different than that of bulk material because of the changes in the location of the band edges.

In this paper, we report the characterization of a Q-particle film prepared by the self-assembly technique[7] by using STM, TS, and PEC measurements. We show here that the E_g of a Q-CdS particle layer is larger than that of a bulk CdS thin film by TS. We also show that V_{on} of a Q-CdS particle layer is more negative than that of a bulk CdS film and that V_{on} for a Q-CdS particle layer, as determined by PEC, correlates with particle size.

Experimental Section

Chemicals and Materials. High-purity water (Millipore purification system, >18 MΩ·cm) was used in the preparation of all solutions. All chemicals were reagent or spectrographic grade and were used as received.

1. Preparation of Q-CdS Particles. Cadmium sulfide particles were prepared in inverse micelles following the methods of Steigerwald et al.[23] Typically two separate solutions, both containing 250 mL of spectrographic grade heptane (Mallinckrodt Specialty Chemicals Co., Paris, KY) and 22.2 g of dioctyl sulfosuccinate (AOT) (Aldrich Chemical Co., Milwaukee, WI), were prepared under argon. To one solution (A), 7.2 mL of 0.4 M $Cd(ClO_4)_2 \cdot 6H_2O$ (Alfa, Ward Hill, MA) aqueous solution was added. To the other solution (B), 7.2 mL of 0.3 M $Na_2S \cdot 9H_2O$ (EM Science, Gibbstown, NJ) (deoxygenated aqueous solution) was introduced. Both solutions were stirred vigorously for >1 h. Solution A was then added very slowly to solution B under argon in the dark. This mixture

[⊗] Abstract published in *Advance ACS Abstracts*, June 15, 1995.

0022-3654/95/2099-11182$09.00/0

SCHEME 1: Schematic Diagram of the Film Formation

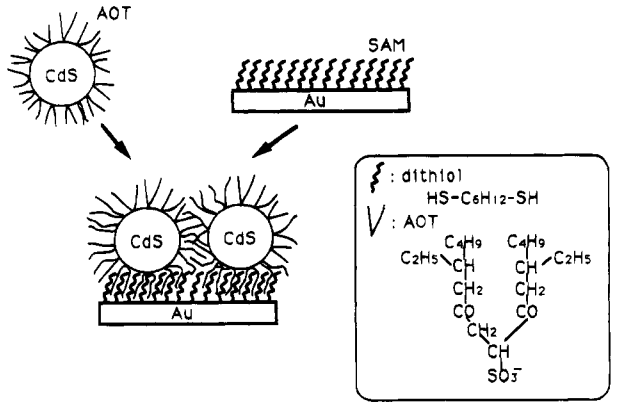

was stirred under argon in the dark for 1 h. The resulting solution was clear and only slightly yellowish. The solution was stored under argon in the dark at room temperature. The CdS particle size was controlled by the ratio $[H_2O]/[AOT]$ in solution.[23]

2. Preparation of Gold Substrates. *A. Sputtered Gold Substrates.* The gold substrates were prepared by sputtering gold (thickness, ~200 nm) on freshly cleaved mica. After sputtering, the gold layers on mica were annealed in a 1×10^{-6} Torr vacuum at 400 °C for about 3 h. Before use, the gold surfaces were cleaned with hot chromic acid [saturated $K_2Cr_2O_7$ (Fisher Scientific; Fair Lawn, NJ) in 90% H_2SO_4 (EM Science)] solution for 30–60 s and then rinsed with copious amounts of water. This process was repeated until the surface contact angle between water and the gold surface was less than 20° (typically between 8° and 16°), indicating that the gold surface was clean.

B. Facets on Gold Balls. Facets on gold balls were prepared by melting 0.5 mm gold wire (Aldrich, 99.99%) in a hydrogen/oxygen flame.[24] The gold balls were cooled to room temperature in air, yielding balls with observable gold (111) facets. The diameter of the resulting gold ball was usually about 1.5 mm. The same cleaning method as with the sputtered gold surfaces was employed before use.

3. Preparation of Dithiol Monolayers on Gold. A 5 mM hexanedithiol (Aldrich) solution was prepared in ethanol (Absolute, Midwest Grain Products, Perkin, IL). SAMs were prepared by immersing gold substrates in this hexanedithiol solution for 10–20 h. After immersion, the samples were removed from solution, rinsed with EtOH at least three times, and then dried with a stream of argon.

4. Preparation of Q-CdS Particle Layers. Q-CdS particle layers were prepared by immersing the SAM-covered Au substrate in the heptane solution containing Q-CdS particles described above for 10–20 h. The samples were then rinsed with heptane several times and dried with argon. Scheme 1 is a schematic representation of the film formation procedure. The samples were stored in the dark under vacuum.

5. Preparation of CdS Thin Film. Polycrystalline CdS thin films on indium tin oxide (ITO) were prepared by chemical bath deposition.[25] The thickness of this film was about 100 nm.

Apparatus. *1. STM and TS.* STM images were obtained on a Nanoscope III scanning tunneling microscope (Digital Instruments, Santa Barbara, CA). Bias voltages are reported as the sample vs the tip. For TS, a home-built apparatus was used; detailed procedures for current and differential conductance measurements with this instrument have been described previously.[19] Briefly, during acquisition of current vs voltage (i–V) or conductance vs V (di/dV – V) curves, the distance

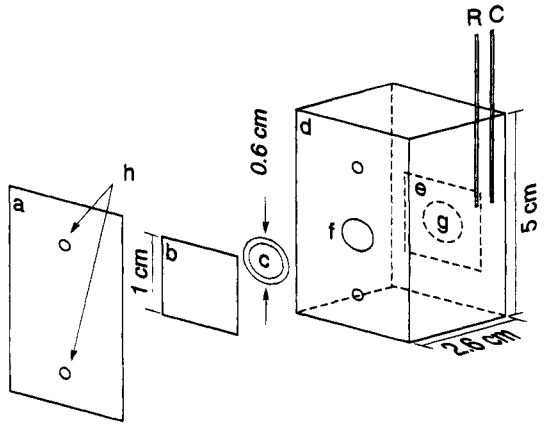

Figure 1. Schematic diagram of the cell used for photoelectrochemical measurements designed so the edges of the electrode are not exposed to the solution: (a) Plexiglas sheet, (b) working electrode, (c) O-ring (0.6 cm diameter), (d) Teflon cell, (e) quartz glass plate, (f) hole exposing the working electrode to the solution, (g) hole exposing the quartz glass plate to the solution, (h) screw holes, (C) counter electrode, (R) reference electrode.

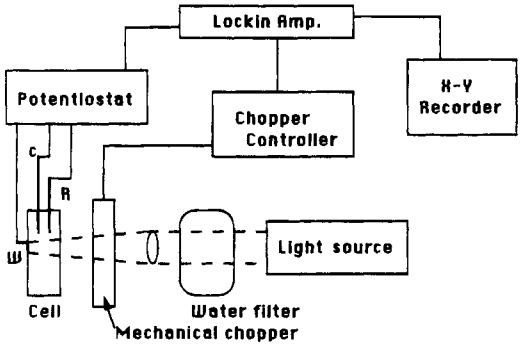

Figure 2. Experimental setup for photoelectrochemical measurements.

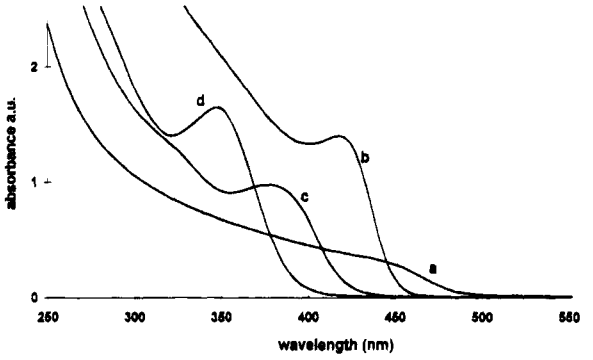

Figure 3. Absorption spectra of Q-CdS particles in heptane solution. The radii were determined by the absorption maximum[26] and the absorption edge. The radii a, b, c, and d were respectively >10, 4, 3, and 2.3 nm.

between tip and substrates was held constant. This was accomplished by gating the feedback control circuit to the z-piezo used for the constant-current mode operation of the STM so that it was active for 1 s between each scan. When the feedback loop was active, a constant voltage superimposed with an ac of 10 mV amplitude was applied to the sample; when inactive, the position of the tip was held stationary at the desired height, and the tunneling current and conductance were measured as a function of bias voltage. Both current and conductance were measured simultaneously at the same location at each bias voltage. Each data point (both i and di/dV) was the average of 20 discrete measurements. Each spectrum reported here was the average of two or three different spectra obtained at the same location. Reproducible spectra could be obtained at

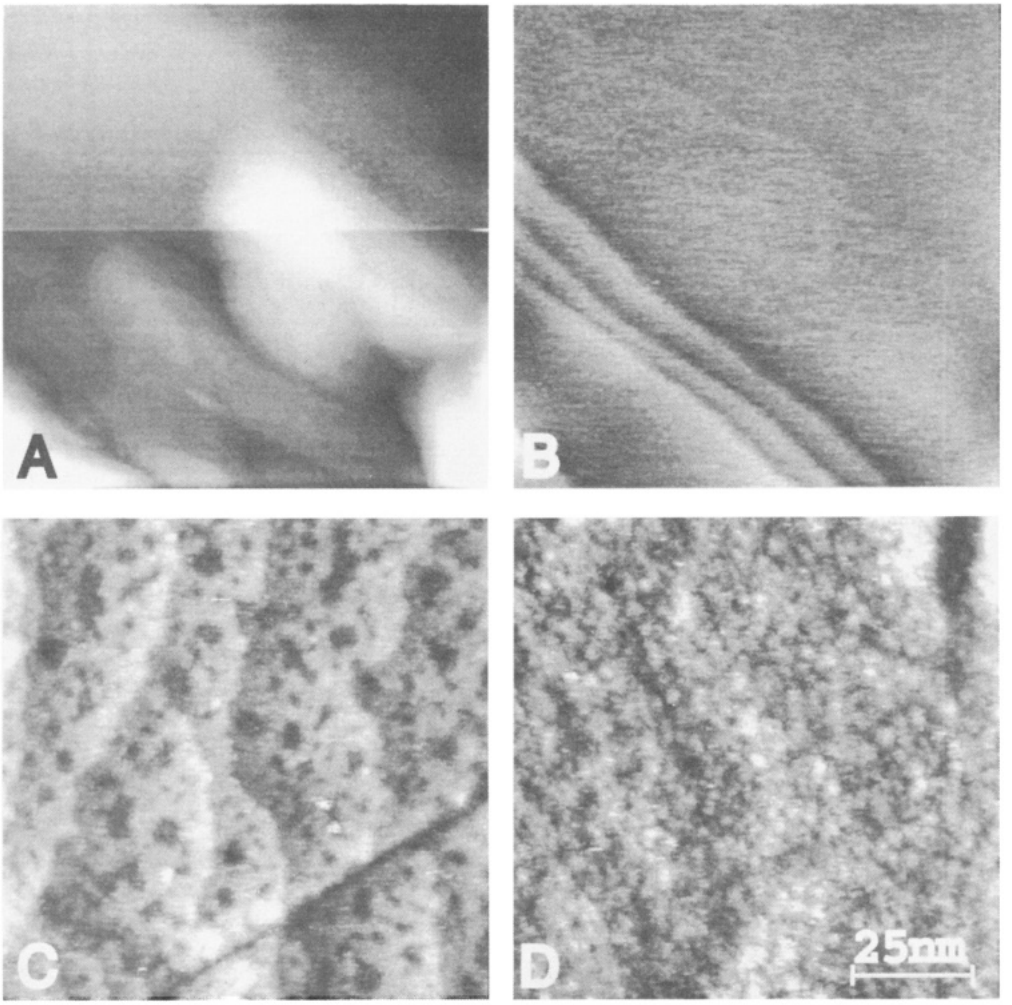

Figure 4. Typical STM image of (A) sputtered gold surface (bias voltage, −0.5 V; current, 0.5 nA), (B) facet of gold ball (0.5 V; 0.5 nA),(C) dithiol/gold surface (−3 V; 0.5 nA), and (D) Q-CdS particle layer on dithiol/gold (−3 V; 0.5 nA).

different locations. The total length of a measurement cycle was a few seconds.

Electrochemically etched Ir−Pt (FHC Co., Brunswick, ME) tips were employed. The TS results reported here were obtained with relatively blunt tips. Sharper tips were used for the STM images. All STM and TS experiments were performed in air.

2. Photoelectrochemistry. The Teflon cell for photoelectrochemical studies, designed to prevent exposure of the edges of the working electrodes to the solution, is shown in Figure 1. The working electrode contacted the solution through a hole in the side wall of the cell and was sealed against the wall with an O-ring, which defined the area exposed to the solution as 0.3 cm^2. A sheet of Plexiglas held by two screws secured the working electrode in the cell wall. The quartz window was similarly sealed through a larger hole in the opposite wall of the cell. A saturated calomel reference electrode (SCE) and a platinum sheet counter electrode, held outside the field of view of the working electrode, were used for all measurements. The solution contained 0.5 M Na_2SO_4 (J.T. Baker, Inc., Phillipsburg, NJ) as the supporting electrolyte and 20 mM triethanolamine (Fisher). All solutions were deoxygenated and had a pH of 9.5. The PEC system is shown schematically in Figure 2. The electrodes were irradiated with a tungsten−halogen lamp (Type 250-T40-CL, Sylvania Electric Products, Fall River, MA) operated to produce an intensity of 5.5 mW/cm^2 at the electrode position. The power of the lamp was determined with a radiometer/photometer (Model 550-1, Princeton Applied Research (PAR), Princeton, NJ). A 17 cm water bath with quartz windows was used to filter out IR. All photocurrent curves were obtained with a potentiostat (Model 173, PAR), a universal programmer (Model 175, PAR), a lock-in amplifier (Model 5210, PAR), a variable frequency light chopper (Model 192, PAR), and an X-Y_1Y_2 recorder (Soltec, Sun Valley, CA).

Absorption spectra were obtained with a Spectronic 3000 array spectrophotometer (Milton Roy Co., Urbana, IL).

Results and Discussion

Film Formation and Characterization. A typical absorption spectrum of Q-CdS particles in heptane solution is given in Figure 3b. The absorbance peak at 424 nm corresponds to an E_g of 2.9 eV and a particle diameter of about 4 nm.[26] This can be compared to the absorption edge of bulk CdS at about 515 nm and an E_g of 2.4 eV. The small shoulder at 360 nm sometimes appears and may result from smaller particles, diameter about 2.6 nm, with $E_g = 3.4$ eV. This sample was used for STM and TS.

Such dispersions of Q-CdS were immobilized on smooth Au substrates and imaged by STM. The goal here was to obtain films with particles held sufficiently strongly to the surface to allow imaging without significant film perturbation because of tip interactions and to record tunneling spectra of individual particles.

Typical STM images of the sputtered gold surface (Figure 4A) and facets of gold balls (Figure 4B) acquired at a typical sample voltage of −0.5 V relative to the tip and a typical reference current of 0.5 nA showed that the gold surfaces, especially the facets on gold balls, were smooth enough to

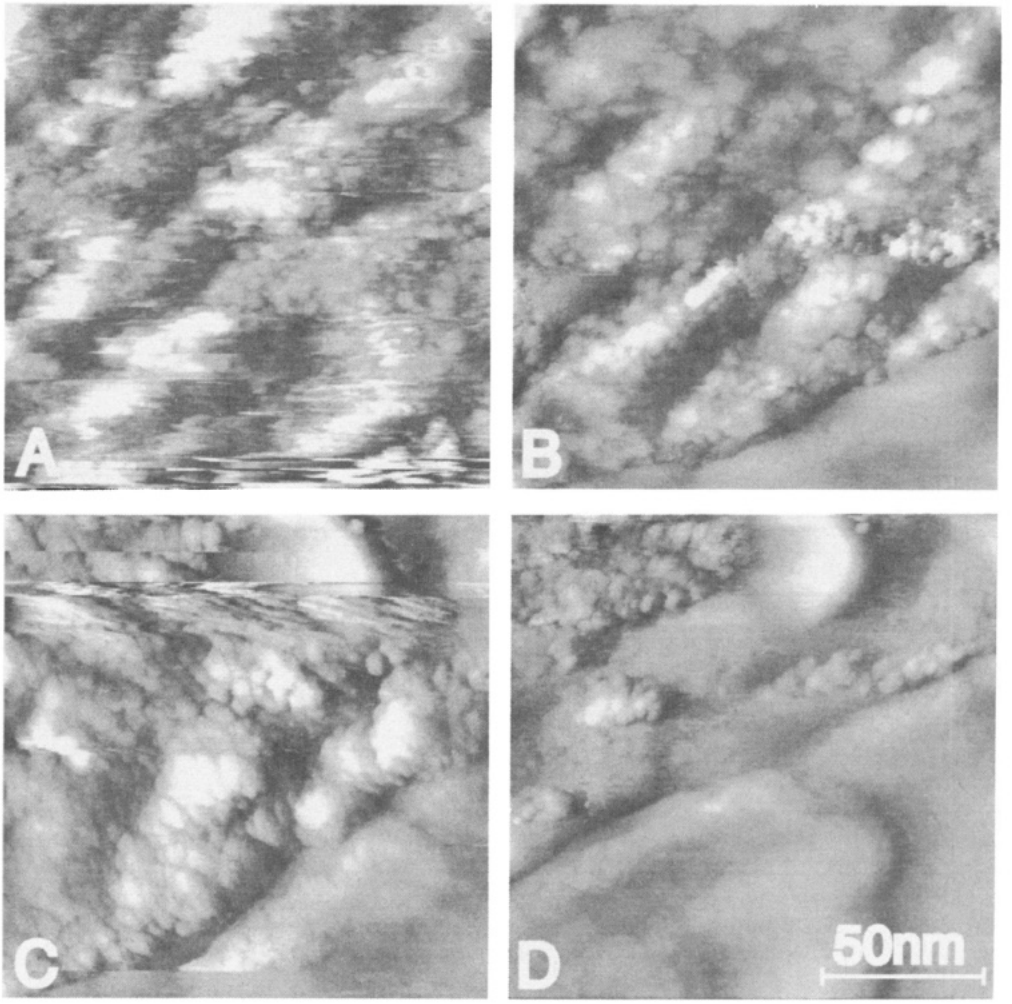

Figure 5. STM images showing the removal of Q-CdS particles by sequential scanning. This sample was a Q-CdS/dithiol/sputtered gold film. Image A was the first image after engagement, acquired at a sample voltage of −3.5 V relative to the tip and a reference current of 0.3 nA. Image B was the third scan image (−2.8 V, 0.3 nA). Images C and D were the fifth and sixth scan images (−1.8 V, 0.3 nA).

observe nanometer size Q-particles on these surfaces by STM. Some gold surfaces had several hundred nanometer terraces and, as in Figure 4B, showed mono- and diatomic steps. While some parts of the sputtered gold surfaces also showed atomic height steps, most images of the sputtered gold surfaces were rougher, as in Figure 4A. Figure 4 also contains typical STM images of a dithiol SAM on gold and a Q-CdS particle layer on the SAM/gold, which were acquired at a typical sample voltage of −3 V relative to the tip and a typical reference current of 0.5 nA. The STM image (Figure 4C) of the dithiol SAM surface on gold showed numerous holes as reported previously.[16b] The STM image in Figure 4D of the Q-CdS particle layer showed that it consisted of uniformly packed particles with diameters of about 4 nm. We could not obtain good STM images under the same imaging conditions for Q-CdS particles cast directly on gold without the dithiol layer. This suggests that the strong interactions between the gold substrate and dithiol and between dithiol and the Q-CdS particles serves to immobilize the particles. High tip bias voltage, low reference current, and a slow tip engagement speed were necessary to obtain good images of the Q-CdS particles. When lower sample bias voltages (0 to −1 V) were used, most Q-CdS particles were moved to the outside of the scan area after the first scan image. Usually after several scans, even at high bias voltage, Q-CdS particles were pushed to the outside of the scan area, indicating that the interaction between Q-CdS particles and dithiol was still not strong enough to prevent particle movement by the tip to allow repetitive imaging of the same area. This tip interaction is illustrated in Figure 5, which shows the removal of Q-CdS particles during sequential scans. Image (A) was the first image, acquired at a bias of −3.5 V and a reference current of 0.3 nA. This noisy image probably results from loosely attached or excess Q-CdS particles on the Q-CdS particle layer surface. Image B, the third scan acquired at a bias of −2.8 V and a reference current of 0.3 nA, was less noisy. Image C, the fifth scan image acquired at a bias of −1.8 V and a reference current of 0.3 nA, shows tip interaction, while the sixth scan, acquired under the same conditions as image C, showed some removal of CdS particles from the surface. As the tip moved closer to the Au surface at smaller bias values, Q-CdS particles were moved to the outside of the images. This could also be seen by imaging a larger area immediately after a series of small-area scans. The size of some of the Q-CdS particles increased with continuous scanning, perhaps because of the aggregation of Q-CdS particles. The series of images in Figure 5 shows a movement in the upper-left direction during scanning because of thermal drift and mechanical relaxation. A similar sequence of STM images with a gold ball substrate is shown in Figure 6. STM images A, B, and C were the first, second, and fourth scan images, acquired at a bias of −2.2 V and a reference current of 0.5 nA. These images also indicated that the Q-CdS particles covered the substrate uniformly and were removed and aggregated with scanning. STM images D, E, and F were the sixth, seventh, and eigthth scan images, acquired at biases of −1.6 V (D), −1.0 V (E), and −0.4 V (F) and a reference current of 0.5 nA. Image F showed that most of the Q-CdS particles

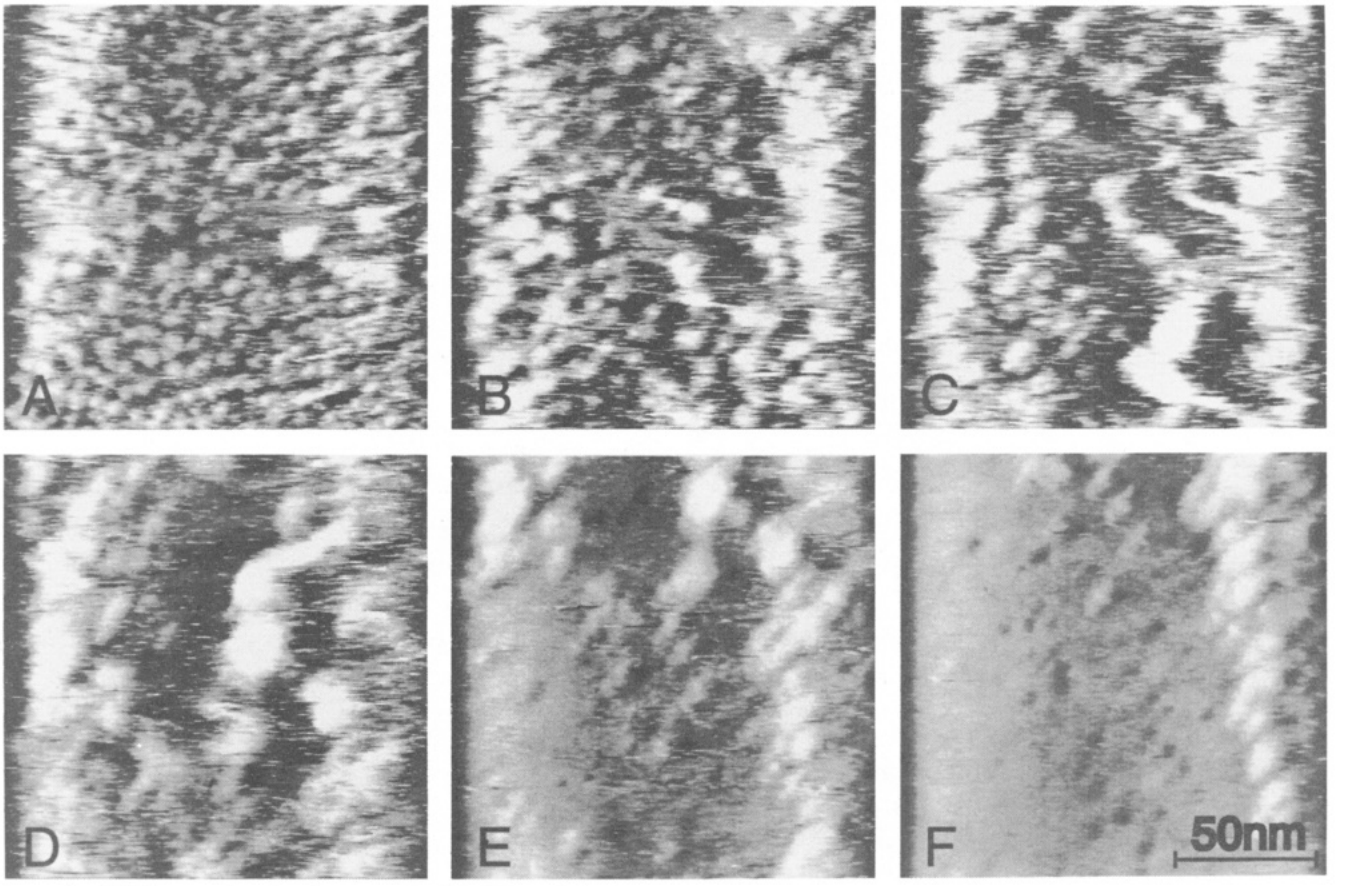

Figure 6. STM images showing the removal of Q-CdS particles by sequential scanning. This sample was a Q-CdS/dithiol/facet of a gold ball. Images A, B, and C were the first, second, and third after engagement, acquired at a sample voltage of −2.2 V relative to the tip and a reference current of 0.5 nA. Images D, E, and F were the sixth, seventh, and eighth, acquired at voltages of −1.6, −1.0, and −0.4 V, respectively, and a reference current of 0.5 nA.

were removed and that many holes similar to those observed on a SAM alkanethiol layer appeared in this image. Clearly in image F most of the CdS layer has been removed, and the underlying gold substrate is uncovered. As the scan continued, these holes became larger. Finally, after extended scanning over this area, the STM image showed a very flat surface with atomic height steps of gold. The results shown in Figures 5 and 6 confirm the structure of the Q-CdS particles within self-assembled dithiol monolayers on gold as reported in Figure 1A in ref 7.

Tunneling Spectroscopy. By recording $i-V$ and di/dV vs V with the tip held close to a semiconductor surface, information about the relative location of band edges and surface state energies can be obtained.[20] Current and differential conductance as functions of voltage of a chemically deposited (bulk) CdS thin film obtained by TS are shown in Figure 7. Since the thickness of this CdS thin film was about 100 nm, its E_g should be similar to that for a bulk CdS crystal. The conductance (di/dV) curve was noisy but clearly showed a wide region of low conductance terminating at two ends in regions of more rapidly rising conductance. This low-conductance region, referred to as the conductance gap, is close to E_g of bulk CdS crystal, about 2.4 eV. Typical current and conductance of a Q-CdS particle layer as functions of voltage and tip−substrate gap separation, S_0, are shown in Figure 8. Here S_0 was determined by the set-point current and voltage used for tunneling gap adjustment. For example, S_0 (−2 V, 30 pA) in the case of (A) was larger than S_0 (−0.5 V, 30 pA) in the case of (B). The di/dV curve of the Q-CdS particle layer in (A) indicates that the E_g for the Q-CdS particle layer is larger than that of the CdS thin film; this is consistent with the quantum size effect of small CdS

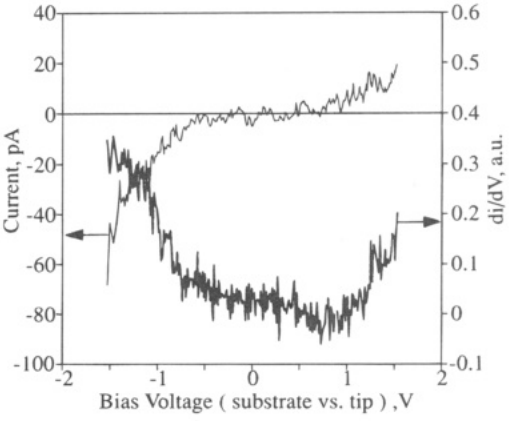

Figure 7. Current and differential conductance as a function of voltage for an Ir−Pt tip and the CdS film. This di/dV curve showed an energy band gap of about 2.3 V.

particles. The conductance gap from Figure 8A is about 3.5 eV, which would correspond to the E_g of the 360 nm absorption shoulder (3.4 eV) as mentioned before. The conductance gap was essentially constant with distance change of ±5 Å with respect to S_0. As the tip moved very close to the substrate at the same location, as in the case of (B), the di/dV curve showed no conductance gap in the low-bias region, and conductance emerged to that of Q-CdS particles as the bias increased. When the tip was close to the substrate, both current and di/dV curves were probably strongly affected by the gold substrate. This di/dV curve would also show contributions from the gold substrate when CdS particles around the measuring point were removed by the tip.

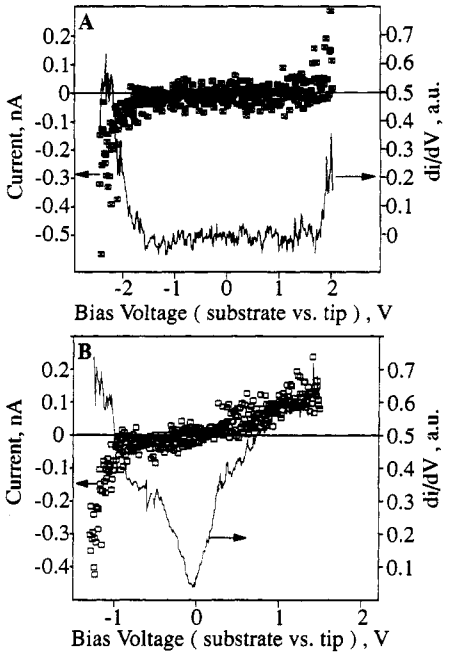

Figure 8. Current and differential conductance as a function of voltage for an Ir−Pt tip and Q-CdS particle layer. The conditions of gap separation between tip and Q-CdS particle layer were (A) −2 V, 30 pA and (B) −0.5 V, 30 pA.

Photoelectrochemistry. PEC experiments involved the recording of current−potential (i−E) curves in the dark and under irradiation for thin-film CdS and layers of Q-CdS particles of different sizes. Such measurements are useful in estimating the location of the conduction band edge from the potential for the onset of photocurrent. Unless otherwise mentioned, triethanolamine (TEA) was used as the hole scavenger in the PEC experiments. With TEA in the solution, the photocurrent of the Q-CdS particle layer was stable for longer than 30 min. Without TEA, the photocurrent decayed within 140 s. One CdS thin film and four different kinds of CdS particle layers were prepared for these PEC measurements. The absorption spectra of four different CdS particle layers are shown in Figure 3. The absorption spectrum edge of sample a was almost the same as that of the bulk CdS thin film; those of samples b, c, and d corresponded to particle sizes of 4, 3, and 2.3 nm, respectively. Figure 9 shows the voltammetric curves under illumination of the CdS thin film and the three different Q-CdS particle layers. Total dc currents of the samples were measured simultaneously with their photocurrents. A lock-in amplifier tuned to the frequency at which the illumination was chopped (50 Hz) was used to discriminate the photocurrent from the dark current. Since the photocurrents were much smaller than the dark currents, except with the bulk CdS thin film, the total currents were essentially equal to the dark currents. In the case of bulk CdS thin film, a separate measurement of the dark current was made, since it was of the same order of magnitude as the photocurrent. The rest potentials of the working electrode in the dark (Figure 10b) and under illumination (Figure 9b) were −0.024 and −0.045 V vs SCE, respectively. As shown in Figure 9, at potentials negative of −1 V, where substantial water reduction occurred, the photocurrent signals were noisy but stable and dependent on the light intensity. The shape of the photovoltammetric curves was independent of the chopping frequency of the light source and intensity, although the detailed structure of the curve on the first scan was sometimes different from that of the subsequent scans. As clearly shown in this figure, layers with smaller Q-CdS particles showed a negative onset V_{on}. It is interesting to compare the difference of the V_{on}

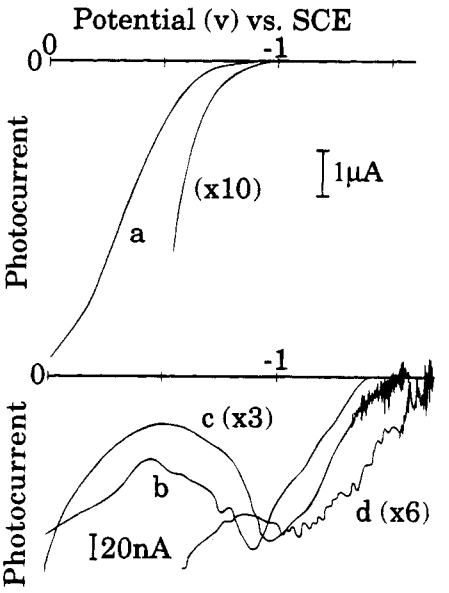

Figure 9. Photocurrent−potential curves of (a) CdS thin layer, (b) 4 nm CdS particle layer, (c) 3 nm CdS particle layer, and (d) 2.3 nm CdS particle layer. The solution contains 20 mM triethanolamine in 0.5 M Na_2SO_4. Potential scan rate is 2−5 mV/s and light intensity is 5.5 mW/cm^2. A phase-sensitive technique was used to monitor the photocurrent. Chopping frequency of light is 50 Hz and lock-in amplifier time constant is 1−3 s.

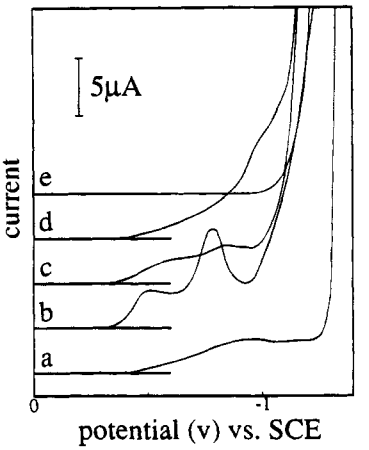

Figure 10. Dark current−potential curves of (a) CdS thin layer on ITO, (b) 4 nm CdS particle layer, (c) 3 nm CdS particle layer, (d) 2.3 nm CdS particle layer, and (e) dithiol SAM.

between the Q-CdS particle layer and the bulk CdS thin film, ΔV_{exp}, with the difference between the conduction band edge of the CdS particle layer and that of the CdS thin film calculated theoretically by the tight binding method,[26] ΔV_{cal}. The linear relation between ΔV_{exp} and ΔV_{cal} as shown in Table 1 suggests that the more negative V_{on} values of the smaller particles are related to their higher conduction band edges.

The shape of the photovoltammetric curves are interesting and different than that usually seen in semiconductor electrodes. First, unlike bulk CdS thin films, which only showed a monotonically increasing photocurrent with increasing potential, the photocurrent of the Q-CdS particle layers showed a peak (with shoulders) near ca. −1 V vs SCE. The position of the peak, like V_{on}, shifted to more negative potentials as the size of the particle became smaller. Following the peak, the photocurrent (as with bulk CdS) increased again with increasing bias potential. Second, the shape of the photocurrent peaks was not strongly dependent on the size of the particle in the range studied (2−10 nm) while the height of the photocurrent peak increased with increasing particle size, as predicted with increasing extent

TABLE 1: Summary of the Onset Potential of CdS Samples

sample no.	absorption peak (nm)	E_g band gap[a] (eV)	diameter[a] (nm)	V_{on}[b] (V)	ΔV_{exp}[c] (V)	ΔV_{cal}[d] (V)
thin film		~2.4*		−1.0	0	0
a[e]	515*	2.4*	>10	−1.0	0	0
b	424	2.92	4	−1.38	0.38 ± 0.04	0.28 ± 0.03
c	381	3.25	3	−1.55	0.55	0.47 ± 0.06
d	348	3.56	2.3	−1.68	0.68	0.61 ± 0.08

[a] Determined by the absorption maximum.[26] (*Band gap and diameter of the sample were estimated by the absorption edge because no peak was shown in the absorption spectra.) [b] The onset potentials are shown in Figure 9. [c] ΔV_{exp} is the difference of the onset potential between the CdS particle layer sample and the bulk CdS sample (thin layer). [d] ΔV_{cal}, which was derived from Figure 1 in ref 26, is the difference between the conduction band edge of the CdS particle and the bulk CdS. [e] Sample a was made by using CdS heptane solution as in Figure 3a.

SCHEME 2: Schematic Energy Diagrams of the Interface between the Electrolyte and CdS Particle Layer in This System

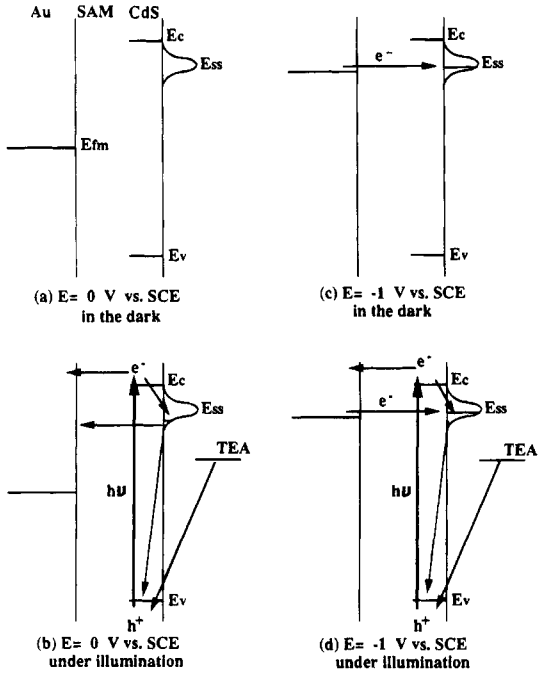

of absorption of light. Third, parallel to the anodic photocurrent peaks observed in the case of the Q-CdS particle layer, the corresponding dark currents also showed similar cathodic peak structures (see Figure 10). These observed results can be interpreted by the model for charge transfer at a metal/insulator/semiconductor/electrolyte junction as shown in Scheme 2, although further studies are required for quantitative analysis. In Scheme 2, the detailed structure of the energy levels of the Q-CdS particle layer is simply represented as the conduction band edge, E_c, and the valence band edge, E_v. There is also surface state, E_{ss}, near E_c, which is arbitrarily represented as a Gaussian distribution. Concerning the origin of the surface states, possible candidates are Cd(II) sites attributable to excess Cd^{2+} used in the preparation of Q-CdS particles, as suggested by Zhao et al.[14] They might also involve less sulfide-coordinated surface CdS species. For simplicity, we have also neglected the reorganization energies involved in the electron-transfer process.[27] Several interesting conclusions can be drawn from this model based on the information shown in Figures 9 and 10. First, at potentials well positive of −0.5 V vs SCE, e.g., 0 V as shown in Scheme 2a, no significant reduction current is observed in the dark, since the Fermi level of Au, E_{fm}, is positive of E_{ss} and E_c. The observed anodic photocurrent at this potential is mainly associated with collection of electrons following oxidation of TEA by the photogenerated holes from the valence band of CdS particles (see Scheme 2b). Second, at potentials negative of −0.5 vs SCE, significant cathodic currents were observed in the dark; these might be attributed to the reduction of the Q-CdS particles and the adsorbed species, e.g., excess Cd(II) sites, as well as water when the potential is well negative of −1.0 V (see Scheme 2c). Under illumination, the photogenerated holes on CdS oxidize TEA while the photogenerated electrons may be trapped efficiently at surface states, which might decrease the EC reduction current. Thus, we have a decreased dark reduction current in addition to the anodic photocurrent due to the oxidation of TEA. This accounts for the anodic photocurrent peak associated with the location of the surface states, as predicted by this model.

Conclusion

We have demonstrated that a layer of Q-CdS particles on an electrode can be prepared by incorporation into a self-assembled dithiol monolayer on gold. The layer consists of a uniformly packed structure as imaged by STM. The energy band gap of the Q-particle was shown to be larger than that of bulk material by tunneling spectroscopy and corresponded to the value derived from the absorption spectrum. The onset potential of Q-CdS particles obtained by PEC techniques was more negative than that of a bulk CdS thin film.

Acknowledgment. The support of this research by grants from Asahi Chemical Industry Co., Ltd., and the National Science Foundation (CHE9119851) is gratefully acknowledged. We thank Mr. Mark F. Arendt for sputtering the gold on mica and Mr. Huajun Tang for the CdS thin film. We appreciate the helpful suggestions by members in our group.

References and Notes

(1) *Semiconductor Electrodes*; Finklea, H. O., Ed.; Studies in Physical and Theoretical Chemistry; Elsevier: Amsterdam, 1988; Vol. 55.
(2) Zhao, X. K.; Xu, S.; Fendler, J. H. *Langmuir* **1991**, *7*, 520.
(3) Zhao, X. K.; Xu, S.; Fendler, J. H. *J. Phys. Chem.* **1991**, *95*, 3716.
(4) Kotov, N. A.; Meldrum, F. C.; Wu, C.; Fendler, J. H. *J. Phys. Chem.* **1994**, *98*, 2735.
(5) Hotchandani, S.; Bedja, I.; Fessenden, R. W.; Kamat, P. V. *Langmuir* **1994**, *10*, 17.
(6) (a) Henglein, A. In *Topics in Current Chemistry*; Springer-Verlag: Berlin, 1988; Vol. 143, pp 113−180. (b) Andres, R. P.; Averback, R. S.; Brown, W. L.; Brus, L. E.; Goddard III, W. A.; Kaldor, A.; Louie, S. G.; Moscovits, M.; Peercy, P. S.; Riley, S. J.; Siegel, R. W.; Spaepen, F.; Wang, Y. *J. Mater. Res.* **1989**, *4*, 704.
(7) Colvin, V. L.; Goldstein, A. N.; Alvisatos, A. P. *J. Am. Chem. Soc.* **1992**, *114*, 5221.
(8) Giersig, M.; Mulvaney, P. *Langmuir* **1993**, *9*, 3408.
(9) Hodes, G.; Albu-Yaron, A.; Decker, F.; Motisuke, P. *Phys. Rev. B* **1987**, *36*, 4215.
(10) (a) Cerdeira, F.; Torriani, I.; Motisuke, P.; Lemos, V.; Decker, F. *Appl. Phys. A* **1988**, *46*, 107. (b) Hodes, G.; Howell, I. D. J.; Peter, L. M. *J. Electrochem. Soc.* **1992**, *139*, 3136.
(11) Dabbousi, B. O.; Murray, C. B.; Rubner, M. F.; Bawendi, M. G. *Chem. Mater.* **1994**, *6*, 216.
(12) Peng, X.; Zhang, Y.; Yang, J.; Zou, B.; Xiao, L.; Li, T. *J. Phys. Chem.* **1992**, *96*, 3412.
(13) Bulhões, L. O. S.; Obeng, Y. S.; Bard, A. J. *Chem. Mater.* **1993**, *5*, 110.
(14) Zhao, X. K.; McCormick, L.; Fendler, J. H. *Chem. Mater.* **1991**, *3*, 922.

(15) Zen, J.-M.; Fan, F.-R. F.; Chen, G.; Bard, A. J. *Langmuir* **1989**, *5*, 1355.

(16) (a) Whitesides, G. M. *Chimia* **1990**, *44*, 310. (b) Kim, Y.-T.; Bard, A. J. *Langmuir* **1992**, *8*, 1096. (c) Widrig, C. A.; Alvis, C. A.; Porter, M. C. *J. Am. Chem. Soc.* **1991**, *113*, 2805. (d) Bucher, J.-P.; Santesson, L.; Kern, K. *Langmuir* **1994**, *10*, 979.

(17) E.g.: Hamers, R. J. In *Scanning Tunneling Microscopy and Spectroscopy—Theory, Techniques and Applications*; Bonnell, D. A., Ed.; VCH: New York, 1993, Chapter 4.

(18) Feenstra, R. M.; Stroscio, J. A.; Fein, A. P. *Surf. Sci.* **1987**, *181*, 295.

(19) Feenstra, R. M.; Stroscio, J. A.; Tersoff, J.; Fein, A. P. *Phys. Rev. Lett.* **1987**, *58*, 1192.

(20) (a) Fan, F.-R. F.; Bard, A. J. *J. Phys. Chem.* **1990**, *94*, 3761. (b) Fan, F.-R. F.; Bard, A. J. *J. Phys. Chem.* **1991**, *95*, 1969. (c) Fan, F.-R. F.; Bard, A. J. *J. Phys. Chem.* **1993**, *97*, 1431.

(21) Zao, X. K.; McCormick, L.; Fendler, J. H. *Langmuir* **1991**, *7*, 1255.

(22) Hoyer, P.; Eichberger, R.; Weller, H. *Ber. Bunsen-Ges. Phys. Chem.* **1993**, *97*, 630.

(23) Steigerwald, M. L.; Alivisatos, A. P.; Gibson, J. M.; Harris, T. D.; Kortan, R.; Muller, A. L.; Thayer, A. M.; Duncan, T. M.; Douglass, D. C.; Brus, L. E. *J. Am. Chem. Soc.* **1988**, *100*, 3046.

(24) Schmidt, L. D. *CRC Crit. Rev. Solid State Mater. Sci.* **1978**, *7*, 129.

(25) Britt, J.; Ferekides, C. *Appl. Phys. Lett.* **1993**, *62*, 31.

(26) Lippens, P. E.; Lannoo, M. *Phys. Rev. B* **1989**, *39*, 10935.

(27) Gerischer, H. In *Advances in Electrochemistry and Electrochemical Engineering*; Delahay, P., Ed.; Interscience: New York, 1961; Vol. 1, Chapter 4.

JP950510T